Confocal Raman Microscopy of the Interfacial Regions of Liquid Chromatographic Stationary Phase Materials

Jennifer L. Gasser-Ramirez and Joel M. Harris*

Department of Chemistry, University of Utah
315 South 1400 East, Salt Lake City, Utah 84112-0850

Abstract

The influence of organic modifiers on the structure of reversed-phase liquid chromatographic (RPLC) stationary phases has been a topic of considerable investigation. Retention of organic modifiers in the stationary phase has previously been determined by chromatographic measurements, and the polarity and heterogeneity of the resulting solvation environment has been studied using solvatochromic, fluorescent, and spin probes. In the present work, the composition and solvation environment of a stationary phase is investigated using confocal Raman microscopy, which allows the *in situ* examination of the solvation environment within individual chromatographic stationary phase particles without the use of probe molecules. The accumulation of organic modifiers in the stationary phase can be quantified and the environment of the modifier in the stationary phase can be determined. Specifically, we have investigated the interactions of acetonitrile with C_{18}-functionalized silica particles using confocal Raman microscopy, which enables the sampling of small (~1fL) volumes within individual 10-μm particles. Bare chromatographic silica was also studied in order to investigate the interactions of acetonitrile with surface silanols. The nitrile-stretching (ν_{CN}) frequency of acetonitrile responds sensitively to the dipolarity of its local microenvironment. The populations of solution-phase and interfacial acetonitrile are thus spectroscopically distinguishable. Scattering from ν_{CN} shows contributions from three different environments within a single RPLC chromatographic particle: acetonitrile in the interparticle mobile phase, C_{18}-chain associated acetonitrile, and acetonitrile that is interacting with residual surface silanols. Data are presented quantifying these populations and characterizing their environments within single stationary phase particles.

*Corresponding author: harrisj@chem.utah.edu

INTRODUCTION

Reversed-phase liquid chromatography (RPLC) utilizes high surface area, xerogel support materials, most often silica, covalently functionalized with n-alkane chains, typically C_{18}, to produce highly porous, non-polar, high surface area stationary phases[1-3]. The interface between the stationary phase and mobile phase plays a critical role in the retention of solutes, and thus has been the subject of many studies designed to understand the structure of the interface and its influence on the interfacial behavior of solutes. Modification of the interfacial environment by mobile phase additives has been studied by chromatographic methods that were used to determine the extent of accumulation of organic modifiers in the stationary phase or stationary phase/solution interface[4-8]. The resulting interfacial environment comprising the silica surface, alkyl chains, and organic modifier has been investigated spectroscopically using solvatochromic[9-15], fluorescence[16-21], and ESR[22, 23] probe molecules. These probe molecules are retained in the stationary phase and report the dipolarity, mobility, and mobile-phase accessibility of their surroundings, reflecting changes in the interfacial environment consistent with accumulation of organic modifier within the n-alkane layer or at the n-alkane-solution interface.

Vibrational spectroscopy is an effective method to investigate the composition and structure of the stationary phase-solution interface without requiring the addition of probe molecules to the sample to report the interfacial environment. Infrared spectroscopy has been employed to investigate changes in alkyl-chain conformation of a n-alkane chain modified stationary phases in response to changes in temperature and exposure to polar and nonpolar solvents solutions[24-26]. Significant gauche defects were observed in the alkyl chains, reflecting chain disorder even at low temperatures; exposure to methanol-water solutions increased the

apparent chain ordering to a small extent. Raman spectroscopy is better suited to the characterization and analysis of RPLC stationary phases, because the Raman scattering from water and silica is weak and does not interfere with the observation of vibrational spectra from the C_{18} chains or organic modifiers. While Raman scattering is a weak effect, it is successfully applied to interfacial studies of chromatographic stationary phases due to the high specific surface area of porous silica supports. The earliest application of Raman spectroscopy to characterize RPLC stationary phases was reported by Ho and Pemberton[27], who showed that the C-C and C-H stretching modes in the 800-1400 and 2700-3100 cm^{-1} regions, respectively, are sensitive to the conformational disorder of the bonded alkane chains, which was applied to investigating the structure of dry C_{18} stationary phases[27]. Further studies by the Pemberton group reported the effects of pure solvents [28-31] on the conformational order of RPLC stationary phases, where polar solvents were found to generate little or no effect on the conformational order of RPLC stationary phases, while non-polar solvents, such as benzene or hexane significantly disrupt the conformation order compared to dry materials. Similarly, Doyle *et al.*[32, 33] used Raman spectroscopy to examine the effects of temperature and exposure to pure solvents: water, acetonitrile, methanol, and chloroform, on the conformational order of RPLC stationary phase chains. It was found, through subtraction of bulk solvent spectra, that the exposure to different solvents did not significantly influence the conformational order of the bonded alkyl chains. The results did show, however, that scattering from acetonitrile and methanol in a packed bed of RPLC stationary phase could be resolved into a signal from bulk liquid solvent molecules and from an interface-associated population.

The results from chromatographic, spectroscopic, and theoretical studies of RPLC systems suggest that the mobile phase composition at the interface of the n-alkane chain

stationary phase is significantly different from that of the bulk mobile phase and should thus influence retention. Chromatographic studies have shown that in equilibrium with aqueous mobile phase solutions, the RPLC stationary phase is enriched with organic modifiers including methanol, acetonitrile, or tetrahydrofuran[4-8]. This behavior is expected because association of the organic modifier with the non-polar alkane chains can lower the interfacial free energies between the non-polar alkane chains and the polar aqueous solution phase [4, 6, 9, 34, 35]. Consistent with this model, Monte-Carlo simulations have also predicted that there is an interfacial excess of organic modifier adsorbed from aqueous mobile phase solutions and associated with the C_{18}-solution interface[36, 37]. These simulations also predict that adsorbed organic modifier accumulates at the silica surface of C_{18} functionalized silica, and that the behavior of this population is consistent with its adsorption onto bare silica[36].

Experimental characterization of the enrichment of organic modifiers in an RPLC stationary phase and the resulting microenvironments local to the stationary phase interface can improve our understanding of solute retention. Because spectroscopic probe molecules for solvatochromic, fluorescence, or ESR measurements are comparable in size to the stationary phase layer and are only capable of reporting the environment in which they reside upon sorption. The goal of the present research, therefore, is to develop Raman spectroscopy as a quantitative method to resolve populations of organic modifier present at the RPLC-solution interface as a function of mobile-phase composition. This goal would be difficult to achieve with measurements on a packed bed of bulk, stationary phase due to the significant (and variable) volume of mobile phase between the particles that interferes with resolving and quantifying the interfacial population. To avoid this problem, we employ confocal Raman microscopy[38-40] to analyze the interior composition of individual RPLC stationary phase

particles. Confocal Raman microscopy employs epi-illumination of the sample with a tightly focused laser beam and imaging of the scattering from the focused spot through a confocal aperture; these optics provide three dimensional spatial resolution of a femtoliter sampling volume, which minimizes background signal contributions from the surrounding sample. When applied to examining individual, C_{18}-derivatized stationary phase particles, the composition of the interior volume of the porous particle can be selectively sampled. Due to the small dimensions of the interparticle pores, this interior volume is dominated by the interface allowing the changes in the composition of the interfacial components to be detected. Confocal Raman microscopy has previously been used to monitor surface binding reactions in porous silica particles[40], where sub-monolayer surface populations were readily detected. The capability of confocal Raman microscopy to sample selectively the interior volume of small particles has also been modeled and demonstrated [41], where the lateral spatial resolution was shown to be 600-nm diameter and the axial resolution was ~1 μm. This capability has been employed to monitor the time-dependent distribution of a solvent permeating an individual polymer colloid[42]. In the present work, we harness these capabilities to determine the composition of interfacial acetonitrile within single, RPLC stationary-phase particles and spectrally resolve populations of acetonitrile in the C_{18} interfacial layer.

EXPERIMENTAL SECTION

Reagents and materials. Acetonitrile (Chromasolv Plus, ≥99.9%) was obtained from Sigma-Aldrich (St. Louis, MO) and was stored over dry molecular sieves and used without further purification. Quartz-distilled water was deionized using a Barnstead NANOpure II (Boston, MA) system. The water had a minimum resistivity of 18.0 MΩ-cm. C_{18}-functionalized and end-capped chromatographic silica was from Phenomenex (Luna C18(2)) and had an average particle diameter of 10 μm, a specific surface area of 400 m^2/g, and a pore diameter of 10 nm. The bonded phase coverage was 3.0 μmole/m^2, with a 17.5% carbon loading. Bare chromatographic silica particles (Luna Silica(2)) were also obtained from Phenomenex to provide a comparable, unfunctionalized material to study mobile phase interactions with the silica support surface.

Confocal Raman microscope. The inverted, confocal Raman microscope used for this study has been described previously[40]. Briefly, a Kr^+ laser beam (Innova 90, Coherent Inc.) operated at 647.1 nm and 50-mW output power. Three mirrors directed the beam to a band-pass filter (F10-647.1-4, CVI Laser Corp.), then through a 4x beam expander (model 50-25-4X-647, Special Optics Inc.), which was mounted on an inverted fluorescence microscope frame (TE 300, Nikon). The expanded laser beam was then directed through a second band-pass filter (D647/10, Chroma Tech Inc.) and reflected into the objective by a dichroic beam splitter (655DCLP, Chroma Tech Inc.). The expanded beam had a power of 22 mW, as it was directed into a 100x oil immersion 1.4 NA microscope objective (CFL PLAN APO, Nikon Inc.), which focused the beam to a 0.6 μm diameter spot in the sample. Raman scattering from the sample was collected and collimated by the same objective and passed through the dichroic beam splitter and a high pass filter (E660LP, Chroma Tech Inc.); the scattering was further filtered by a 647-nm

holographic notch filter (Kaiser). The confocal aperture was realized by focusing the Raman scattered light through a 50-μm monochromator slit (500IS, Bruker), which defined the horizontal dimension of the aperture. Binning 3 rows of pixels of the charge-couple device (CCD) camera (DV420, Andor Inc.) limited the vertical dimension to 78 μm. Spectra were dispersed with either a 300 lines/mm or 600 lines/mm diffraction grating, both blazed at 750 nm, yielding a spectral resolution of 6 cm^{-1} or 3 cm^{-1}, respectively. Particle images were acquired with a digital camera (CoolPix 950, Nikon, Inc.).

Sample preparation and collection of spectra. Because C_{18} derivatized particles do not spontaneously wet in highly aqueous mobile phases[43], the particles were dispersed initially in pure acetonitrile. Aliquots of this dispersion were then diluted with deionized water to obtain final acetonitrile concentrations ranging from 0.002 to 1.0 mol-fraction acetonitrile. Small aliquots (50 μL) of these particle dispersions were transferred into a microscopy sample cell, which was constructed by attaching a 1-cm length of glass tubing (o.d. = 0.5 cm, i.d. = 0.3 cm) to the surface of a cover slip with epoxy. Raman spectra were acquired from individual, 10-μm particles by centering the particle of interest over the laser focus using the x-y microscope stage controller. The objective was then raised 5 μm in the z direction, so that the laser focus and confocal collection volume were located in the center of the particle. Each Raman spectrum was acquired for two minutes; a dark-background offset was subtracted from the data, and the net intensities were ratioed to a white light detector response using procedures implemented in Matlab (MathWorks)[44]. Baseline subtraction was performed by fitting a fifteen point cubic spline to points along the baseline and subtracting this fitted function from the spectral data prior to analysis.

RESULTS AND DISCUSSION

Confocal Raman microscopy of individual chromatographic silica particles. Raman spectra were acquired from individual, 10-μm silica particles by translating the microscope stage in the x,y direction until a particle of interest was centered over the laser focus. An example bright-field image of several chromatographic support particles is shown in Figure 1a, with the excitation laser beam reflected from the cover slip below one of the particles near the center of the image. The microscope objective was then translated 5 μm upward in the z direction, such that the laser focus and focal plane of the microscope were located approximately in the center of the chromatographic particle, as illustrated in Figure 1b. Notice that as the focal plane coincides with the middle of the particle, the perimeter of the particle comes into much sharper focus (compare with Figure 1a). While the silica material is highly porous where one might anticipate significant loss of image fidelity due to scattering, it is evident from Figure 1b that the integrity of the focused beam is well maintained at the center of the particle. This is not a surprising result, however, because the 10-nm silica pores are much smaller than (0.015-times) the wavelength of the excitation light, and the refractive index difference between the silica and the acetonitrile/water solutions is also small, ~8%. This result assures that the Raman scattering is excited and collected from a small (~fL) volume at the center of the chromatographic particle with no interference from the inter-particle solution and improves the quantitative reproducibility of the detecting interfacial populations.

An example Raman scattering spectrum acquired from the center of a single C_{18}-modified silica particle, equilibrated for one hour with a 0.03-mol fraction acetonitrile solution, is shown in Figure 2. From these results, it is evident that Raman scattering from the C_{18} chains bound to the surface of the silica particle is readily detected, with both methylene and methyl C-H

stretching modes and CH_2 bending and twisting modes, as noted in the figure. Raman scattering from acetonitrile and water within the particle is also quite evident, where scattering from the CH (ν_{CH}) and CN (ν_{CN}) stretching vibrations of acetonitrile are observed at 2940 and 2253 cm^{-1}, respectively [45, 46] and the OH stretching from water (ν_{OH}) is found in a broad band between 3100 cm^{-1} and 3500 cm^{-1}, where the band centered around 3200 cm^{-1} corresponds to the symmetric stretch, $\nu_s(OH)$, and the band at around 3450 cm^{-1} corresponds to the antisymmetric stretch, $\nu_a(OH)$[47].

Quantifying organic-modifier concentrations within individual silica particles. The accumulation of acetonitrile in a C_{18}-silica stationary phase can be monitored by detecting the Raman scattering from the interior of individual particles as a function of mobile-phase composition. In Figure 3, Raman spectra are plotted for scattering acquired from C_{18}-stationary phase particles in equilibrium with aqueous acetonitrile solutions, where the acetonitrile concentration is varied from 0.002 to 0.19 mole fraction. The results show that scattering from the C_{18}-alkyl chains remains constant with increasing acetonitrile concentration, as expected, and illustrate the consistent quantitative response between sampled particles. The intensity of scattering from both the ν_{CN} and ν_{CH} modes of acetonitrile increases with the solution concentration of acetonitrile, but the increase in intensity is greater in the particle than in the solution surrounding the particle, suggesting that acetonitrile in the confocal volume is accumulating in the stationary phase[4].

If acetonitrile accumulates preferentially within the C_{18} particles, then its volume fraction relative to water will be locally greater than the surrounding acetonitrile-water mobile phase. The relative Raman scattering intensity from acetonitrile and water should be capable of reporting the fractions of acetonitrile in the stationary-phase and mobile-phase environments. In

order to calibrate the Raman scattering response, Raman spectra were also acquired from the acetonitrile-water solution adjacent to the particles by simply translating the microscope stage laterally until a particle-free region was being sampled by the confocal-volume at the same 5 μm height above the cover slip. From these solution spectra, the scattering intensity under the nitrile stretching (ν_{CN}) band was ratioed to the total scattering from the water OH-stretching bands ($\nu_{s,OH}$ and $\nu_{a,OH}$) *plus* the nitrile stretching (ν_{CN}) intensity, and the results were plotted against the mole fraction of acetonitrile. This intensity ratio corrects for small (<3%) changes in Raman scattering cross section[48] with variation in the refractive index of the surrounding medium. Because the Raman cross sections of these vibrational modes are not equal, the intensity of one of them must be scaled in order for the scattering intensities to predict the mole fractions of the two components. Because the mole fractions of the components in the mobile-phase solutions are known, a scaling factor for the OH-scattering intensity was adjusted until the fractional intensities of the nitrile Raman scattering predict the mole fraction of acetonitrile in the mobile-phase solutions with the least-squared deviations weighted by the variance of the observed ratios (see Figure 4). This same scaling factor (1.88) was then applied to the ν_{OH} band intensities of spectra collected from C_{18}–silica particles as well as from bare silica particles, and results are plotted in Figure 4.

The Raman scattering from the nitrile stretching ν_{CN} is clearly much greater from the C_{18}–silica stationary phase particles than from the mobile phase solution, demonstrating significant enrichment of acetonitrile in the stationary phase. A weighted-least squares fit of the first 10 points to a straight line (no intercept) shows that acetonitrile is present at a 3-fold greater total mole-fraction in the C_{18}–silica particles than in the mobile-phase in which they are immersed. This result indicates a 2-fold surface excess, the magnitude of which is consistent

with isotherm measurements obtained chromatographically[4, 6]. The bare silica particles also exhibit surface enrichment of acetonitrile compared to the bulk solution composition; however, the total mole fraction is increased by a smaller factor of 1.2.

Characterizing the interfacial solvation environment. The above data show that confocal Raman microscopy is capable of quantifying interfacial-excess acetonitrile within a chromatographic support particle. A more unique capability is to characterize the interfacial environment of the acetonitrile by examining frequency shifts of the nitrile stretching mode, ν_{CN}. The frequency of the nitrile stretching mode has been shown to strongly depend on the dipolarity of the surrounding solvation environment[46, 49-51]. In a series of protic solvents, a monotonic increase in the nitrile stretching frequency was observed with increasing dielectric constant, with a maximum shift of 7 cm^{-1} in water [49] compared to the ν_{CN} frequency from pure acetonitrile. Further work in this area[46, 50, 51] has show correlations in the frequency shifts with solute-solvent interactions including dipolarity, dielectric strength, and donor-acceptor properties. Thus, the nitrile stretching frequency can potentially be used to resolve and characterize the local environment of interfacial excess acetonitrile populations. Unlike fluorescence, solvatochromic, or spin probes, the small size of acetonitrile should allow it to report environmental inhomogeneities on a scale smaller than the dimensions of the C_{18}-alkyl chains.

To test this concept, the capability of resolving the small population of acetonitrile adsorbed onto bare silica was determined by comparing the solution-phase spectra of acetonitrile with those gathered from the interior of a bare silica particle (see example in Figures 5a and b). A shift in the center frequency (~1 cm^{-1} to higher frequency) and a comparable increase in the bandwidth are observed for the nitrile stretching band from acetonitrile within the silica particle (Figure 5b). The least-squares best fit of this spectrum to the solution-phase spectrum (by simple

amplitude scaling) showed structured residuals consistent with a shift of the band to higher frequency. The error in the fit was significantly greater than the reproducibility of measuring solution or silica spectra, with a large F-ratio = 37 (n_1 = 14 and n_2 = 27 degrees of freedom), indicating a significant silica-surface contribution to the measured acetonitrile Raman scattering.

To resolve this silica-surface population from scattering by solution-phase acetonitrile in the pores of the silica particle, the average acetonitrile solution spectrum for this composition was subtracted from the total interparticle scattering, where the amplitude of the solution spectrum was adjusted until the spectral intensity in the low frequency region merged with the baseline. The resulting difference spectrum, shown in Figure 5b, exhibits a 2 cm^{-1} higher nitrile-stretching frequency and a somewhat broader bandwidth (5.0 versus 4.3 cm^{-1}) compared to solution-phase acetonitrile. The higher frequency ν_{CN} scattering is consistent with a more dipolar, acidic environment[46, 49] and the greater bandwidth is likely due to the acetonitrile experiencing a greater heterogeneity in environments at the silica surface than in aqueous solution. This environmental heterogeneity is likely due to the diversity of surface silanols[52] (isolated, vicinal, and geminal) giving rise to frequency shifts in the vibrational spectra of adsorbates.[53] The fraction of acetonitrile that is silica-surface associated can be estimated from the scattering intensity of the difference spectrum, which is 30% of the total intensity comparable to the 20% excess in the mole-fraction of acetonitrile in the silica particles determined from the total ν_{CN} scattering relative to the total scattering from ν_{CN} and ν_{OH} (see Figure 4, above).

This same approach can be applied to resolving the component Raman spectra from acetonitrile in C_{18} silica (Figure 5c). To account for bulk solution phase in the pores and the acetonitrile associated with the silica surface, the free-solution acetonitrile spectrum (Figure 5a) and silica-associated acetonitrile spectrum (resolved in Figure 5b) were subtracted from the total

C_{18} interparticle scattering, with the amplitudes adjusted until their contributions merged with the baseline. The resulting difference spectrum (Figure 5c) arises from acetonitrile associated with the C_{18}-alkyl chains; it exhibits a 5.1 cm^{-1} *lower* nitrile-stretching frequency and a slightly greater bandwidth (4.8 versus 4.3 cm^{-1}) compared to solution-phase acetonitrile. The lower frequency ν_{CN} scattering is consistent with a less polar environment[46, 49] and the slightly greater bandwidth is likely due to variation in dipolarity within the C_{18}-silica layer depending on the local infiltration of solvent or proximity to the solution interface. The fraction of acetonitrile that is interface-associated (C_{18} plus silica) can be estimated from the scattering intensities of these two component spectra, and they total twice the intensity of the solution-phase component within the particle. This result agrees with the 2-fold mole-fraction surface-excess acetonitrile, determined from the total ν_{CN} scattering compared to the total scattering from ν_{CN} and ν_{OH} (see above).

This same procedure was repeated for spectra acquired over the full range of acetonitrile concentrations. For bare silica particles, the fraction of acetonitrile scattering that is shifted to higher frequency and associated with the silica surface (distinguishable from the bulk solution spectrum) is plotted versus solution composition in Figure 6. The surface-associated fraction is greatest at low concentrations of acetonitrile, where it appears to preferentially adsorb to surface silanols. This is a somewhat surprising result because acetonitrile is not as strong at hydrogen-bonding compared to water. However, acetonitrile is strongly dipolar (with a more than 2-fold greater dipole moment that water[54]), and its surface association may relate to the silica being polarized by the strong dipole moment[55] and possible dissociation[56] of surface silanols; adsorption of acetonitrile could also lower the energy cost of disrupting the structure of water near the interface[35]. At higher concentrations, the fraction of acetonitrile that is silica-surface

associated lowers to a constant 23% fraction of the solution-phase acetonitrile in the particle, which is consistent with the results in Figure 4 determined from the total acetonitrile scattering compared to water.

For C_{18}-derivatized particles, the association of acetonitrile is much greater over the entire range of solution compositions. The total interface-associated and solution-phase acetonitrile fractions are plotted in Figure 7 as a function of mole fraction of acetonitrile. The data indicate a 1.7-fold greater population of acetonitrile at the interface compared to the interparticle solution fraction, which is close to the 2-fold surface enrichment estimated from the total acetonitrile scattering compared to water (Figure 4). Based on the significant shifts in the nitrile stretching frequencies (see Figure 5, above), the interfacial populations of acetonitrile can be easily resolved into the fractions that associate with surface silanols and the C_{18} chains, respectively. The relative fractions of these two interfacial populations of acetonitrile are plotted in Figure 8 as a function of mole fraction of acetonitrile. At the lowest concentration of acetonitrile, the results show a greater enrichment of acetonitrile at residual surface silanols, similar to the behavior observed on the bare silica particles and suggesting a small population of especially high activity silanols that accumulate acetonitrile at low concentrations. At all concentrations, most of the acetonitrile at the interface is associated with the C_{18} chains, as expected, where acetonitrile accumulates at the C_{18}–solution interface to minimize the interfacial free energy between the C_{18} alkane chains and the aqueous solution phase[4, 6, 9, 34, 35]. This C_{18}–associated fraction of acetonitrile is, on average, 4-times greater than the silica-surface associated population, but while the latter population is smaller, it is clearly present and plays a role in defining the interfacial environment. This acetonitrile population should lower the free energy between the dipolar silica surface and the lower dielectric constant C_{18} chains, analogous to its

role at the C_{18}-solution interface, while the adsorbed acetonitrile would exhibit the strong dipole-dipole interactions with surface silanols. Monte-Carlo simulations of methanol-water solutions in contact with C_{18} chains bound to silica[36] have predicted that two populations of interfacial organic modifier exist, one near the interface between the mobile phase and the alkane chains and another population at the interface between the silica surface and the C_{18} chains. Similar behavior would be expected for acetonitrile, based on Monte-Carlo simulations of a single octadecane chain in contact with acetonitrile solutions[35], with a likely greater association of the organic modifier with the interface to reduce the water-structure breaking effects of acetonitrile[35].

In addition to a quantitative analysis of the interfacial populations of acetonitrile, the Raman microscopy data can also provide information about changes in the interfacial environments of these populations based on shifts in the nitrile stretching frequency[46, 49-51]. The nitrile stretching frequencies of the three populations of acetonitrile are plotted as a function of acetonitrile concentration in Figure 9. The nitrile stretching frequency of solution-phase acetonitrile decreases with increasing acetonitrile concentration as previously described[46, 49], which is attributed to an increasing population of acetonitrile that is free of hydrogen bonding interactions with water[46]. This same trend is evident in the higher frequency ν_{CN} scattering from the silica-associated population, which is consistently in a more dipolar, acidic environment than free solution; with an increasing population of acetonitrile at the silica interface, the silanol-acetonitrile interactions become weaker on average. At all concentrations of acetonitrile, the population of organic modifier associated with the C_{18} interface is found in a less polar environment than the mobile-phase solution, but the average polarity of the C_{18} region decreases with additions of acetonitrile as water is displaced from the interfacial region. The dipolarity

contrast between the interfacial and bulk acetonitrile environments, however, nearly disappears at the highest acetonitrile concentrations, where the accumulated acetonitrile in the C_{18} chains increases and dominates the interfacial environment. Finally, it is interesting to note that the solution-phase acetonitrile within the pores of both bare and C_{18} silica cannot be distinguished from bulk acetonitrile-water mixtures of the same composition. This indicates that beyond the silica- or C_{18}- interface, the dipolarity and hydrogen bonding interactions (which shift the nitrile stretching frequency[46, 49-51]) of the solution within the pores appears to be very similar to the bulk mobile phase. Previous fluorescence-quenching studies have shown that molecular diffusion rates (corrected for pore geometry) in aqueous solutions within both bare[57] and hydrophobic[58] (methylated) silica are equivalent to diffusion in the bulk solvent.

Conclusions. Confocal Raman microscopy has been used to probe the solvation environment within individual C_{18} stationary-phase particles. The femtoliter detection volume confines the observation to the interparticle region and allows quantitative analysis of interfacial solvent populations and their local solvation environments. We have been able to identify and quantify three populations of acetonitrile within the reversed-phase chromatographic particles: a bulk mobile-phase fraction, a C_{18}-associated population, and a fraction that is associated with residual surface silanols. The nitrile stretching frequency of the silanol-associated component indicates that the local environment is much more dipolar than the bulk aqueous solution. The nitrile frequency of the C_{18}-associated acetonitrile is consistent with an interfacial environment that is much less dipolar than the mobile-phase solution. At high concentrations of acetonitrile, however, the environment local to the C_{18} layer exhibits a nitrile stretching frequency nearly the same as bulk acetonitrile, suggesting that the acetonitrile has fully solvated the alkyl chains.

Acknowledgements

The authors thank M. Lei Geng for providing us a sample of the C_{18} stationary-phase particles. This work was supported in part by funds from the U. S. Department of Energy under Grant DE-FG03-93ER14333.

References:

(1) Snyder, L. R.; Kirkland, J. J. *Introduction to modern liquid chromatography* Wiley: New York, 1979.
(2) Giddings, J. C. *Unified Separation Science*; Wiley & Sons, Inc: New York, 1991.
(3) Snyder, L. R.; Kirkland, J. J.; Glajch, J. L. *Practical HPLC method development* John Wiley & Sons: New York, 1997.
(4) McCormick, R. M.; Karger, B. L. *Anal. Chem.* **1980**, *52*, 2249-2257.
(5) Poppe, H. *Journal of Chromatography A* **1993**, *656*, 19-36.
(6) Kazakevich, Y. V.; LoBrutto, R.; Chan, F.; Patel, T. *J. Chromatogr. A* **2001**, *913*, 75-97.
(7) Gritti, F.; Guiochon, G. *Anal. Chem.* **2005**, *77*, 4257-4272.
(8) Gritti, F.; Guiochon, G. *J. Chromatogr. A* **2006**, *1103*, 57-68.
(9) Ying, P. T.; Dorsey, J. G.; Dill, K. A. *Anal. Chem.* **1989**, *61*, 2540-2546.
(10) Jones, J. L.; Rutan, S. C. *Anal. Chem.* **1991**, *63*, 1318-1322.
(11) Lu, H.; Rutan, S. C. *Anal. Chem.* **1996**, *68*, 1387-1393.
(12) Nigam, S.; De Juan, A.; Cui, V.; Rutan, S. C. *Anal. Chem.* **1999**, *71*, 5225-5234.
(13) Nigam, S.; Stephens, M.; De Juan, A.; Rutan, S. C. *Anal. Chem.* **2001**, *73*, 290-297.
(14) Nigam, S.; Rutan, S. *Appl. Spectrosc.* **2001**, *55*, 362A-370A.
(15) Rutan, S. C.; Harris, J. M. *Journal of Chromatography A* **1993**, *656*, 197-215.
(16) Lochmüller, C. H.; Marshall, D. B.; Wilder, D. R. *Analytica Chimica Acta* **1981**, *130*, 31-43.
(17) Carr, J. W.; Harris, J. M. *Anal. Chem.* **1986**, *58*, 626-631.
(18) Carr, J. W.; Harris, J. M. *Anal. Chem.* **1987**, *59*, 2546-2550.
(19) Wirth, M. J.; Ludes, M. D.; Swinton, D. J. *Anal. Chem.* **1999**, *71*, 3911-3917.
(20) Ludes, M. D.; Wirth, M. J. *Anal. Chem.* **2002**, *74*, 386-393.
(21) Zhong, Z.; Geng, M. L. *Anal. Chem.* **2007**, *79*, 6709-6717.
(22) Wright, P. B.; Lamb, E.; Dorsey, J. G.; Kooser, R. G. *Anal. Chem.* **1992**, *64*, 785-789.
(23) Sentell, K. B. *Journal of Chromatography A* **1993**, *656*, 231-263.
(24) Sander, L. C.; Callis, J. B.; Field, L. R. *Anal. Chem.* **1983**, *55*, 1068-1075.
(25) Srinivasan, G.; Neumann-Singh, S.; Muller, K. *J. Chromatogr. A* **2005**, *1074*, 31-41.
(26) Srinivasan, G.; Kyrlidis, A.; McNeff, C.; Muller, K. *J. Chromatogr. A* **2005**, *1081*, 132-139.
(27) Ho, M.; Cai, M.; Pemberton, J. E. *Anal. Chem.* **1997**, *69*, 2613-2616.
(28) Orendorff, C. J.; Ducey Jr., M. W.; Pemberton, J. E.; Sander, L. C. *Anal. Chem.* **2003**, *75*, 3369-3375.
(29) Pemberton, J. E.; Ho, M.; Orendorff, C. J.; Ducey, M. W. *J. Chromatogr. A* **2001**, *913*, 243-252.
(30) Ducey Jr., M. W.; Orendorff, C. J.; Pemberton, J. E.; Sander, L. C. *Anal. Chem.* **2002**, *74*, 5585-5592.
(31) Orendorff, C. J.; Ducey Jr., M. W.; Pemberton, J. E.; Sander, L. C. *Anal. Chem.* **2003**, *75*, 3360-3368.
(32) Doyle, C. A.; Vickers, T. J.; Mann, C. K.; Dorsey, J. G. *J. Chromatogr. A* **2000**, *877*, 25-39.
(33) Doyle, C. A.; Vickers, T. J.; Mann, C. K.; Dorsey, J. G. *J. Chromatogr. A* **2000**, *877*, 41-59.
(34) Martire, D. E.; Boehm, R. E. *J. Phys. Chem.* **1983**, *87*, 1045-1062.

(35) Sun, L.; Siepmann, J. I.; Schure, M. R. *J. Chem. Theory Comput.* **2007**, *3*, 350-357.
(36) Zhang, L.; Rafferty, J. L.; Siepmann, J. I.; Chen, B.; Schure, M. R. *J. Chromatogr. A* **2006**, *1136*, 219-231.
(37) Rafferty, J. L.; Zhang, L.; Siepmann, J. I.; Schure, M. R. *Anal. Chem.* **2007**, *79*, 6551-6558.
(38) Puppels, G. J.; Colier, W.; Olminkhof, J. H. F.; Otto, C.; Mul, F. F. M. d.; Greve, J. *J. Raman Spectrosc.* **1991**, *22*, 217-225.
(39) Williams, K. P. J.; Pitt, G. D.; Batchelder, D. N.; Kip, B. J. *Appl. Spectrosc.* **1994**, *48*, 232-235.
(40) Houlne, M. P.; Sjostrom, C. M.; Uibel, R. H.; Kleimeyer, J. A.; Harris, J. M. *Anal. Chem.* **2002**, *74*, 4311-4319.
(41) Bridges, T. E.; Houlne, M. P.; Harris, J. M. *Analytical Chemistry* **2004**, *76*, 576-584.
(42) Bridges, T. E.; Uibel, R. H.; Harris, J. M. *Anal. Chem.* **2006**, *78*, 2121-2129.
(43) Walter, T. H.; Iraneta, P.; Capparella, M. *J. Chromatogr. A* **2005**, *1075*, 177-183.
(44) Cherney, D. P.; Conboy, J. C.; Harris, J. M. *Anal. Chem.* **2003**, *75*, 6621-6628.
(45) Reitz, A. W.; Skrabal, R. *Monatsh. Chem.* **1937**, *70*, 398-404.
(46) Reimers, J. R.; Hall, L. E. *J. Am. Chem. Soc.* **1999**, *121*, 3730-3744.
(47) Scherer, J. R.; Go, M. K.; Kint, S. *J. Phys. Chem.* **1974**, *78*, 1304-1313.
(48) Veas, C.; McHale, J. L. *J. Phys. Chem.* **1990**, *94*, 2794-2800.
(49) Rowlen, K. L.; Harris, J. M. *Anal. Chem.* **1991**, *63*, 964-969.
(50) Ben-Amotz, D.; Lee, M.-R.; Cho, S. Y.; List, D. J. *The Journal of Chemical Physics* **1992**, *96*, 8781-8792.
(51) Fawcett, W. R.; Liu, G.; Kessler, T. E. *The Journal of Physical Chemistry* **1993**, *97*, 9293-9298.
(52) Iler, R. K.; John Wiley and Sons: New York, NY, 1979.
(53) Rivera, D.; Poston, P. E.; Uibel, R. H.; Harris, J. M. *Anal. Chem.* **2000**, *72*, 1543-1554.
(54) Weast, R. C., Ed. *Handbook of Chemistry and Physics, 62nd Edition*; CRC Press: Boca Raton, FL, 1981.
(55) Wan, Q.; Ramaley, L.; Guy, R. *Chromatographia* **1997**, *46*, 495-500.
(56) Healy, T. W.; White, L. R. *Advances in Colloid and Interface Science* **1978**, *9*, 303-345.
(57) Wong, A. L.; Hunnicutt, M. L.; Harris, J. M. *The Journal of Physical Chemistry* **1991**, *95*, 4489-4495.
(58) Wong, A. L.; Harris, J. M. *The Journal of Physical Chemistry* **1991**, *95*, 5895-5901.

Figure Captions

Figure 1. a) Image of C_{18}–silica stationary phase particles, with the laser focus reflected from the cover slip below the center particle. b) Image of the same C_{18} particles where the microscope objective has been raised 5 μm, so that the laser focus is at the center of the target particle. Note that the perimeter of the particle is now in focus, showing that the focal plane (blue dots in the cartoon on the right) bisects the particle. The scale bar is 10 μm.

Figure 2. Raman spectrum acquired from a single C_{18}-silica stationary phase particle, equilibrated with an aqueous solution containing 0.03 mole fraction acetonitrile. Symmetric (ν_s) and antisymmetric (ν_a) stretching, twisting, and bending (δ) modes of the CH_2 groups of the C_{18} stationary phase are readily detected, along with scattering from the CN, CH stretching (ν) modes of acetonitrile and OH stretching of water.

Figure 3. A series of Raman spectra acquired from individual C_{18}-silica stationary phase particles, equilibrated with aqueous solutions containing 0.002 to 0.19 mole fraction acetonitrile, bottom to top, respectively. These survey spectra are acquired with 6-cm^{-1} resolution.

Figure 4. Raman scattering detection of enrichment of acetonitrile relative to water in chromatographic silica. The Raman scattering from nitrile stretching (ν_{CN}) is ratioed to the total scattering from nitrile and water (ν_{CN} and ν_{OH}), the latter being multiplied by a scaling factor (1.88) to account for the differences in Raman scattering cross sections. Results are plotted for bulk solution (▪), bare silica particles (▲), and C_{18}–silica particles (●). Determination of acetonitrile-enrichment by this method is limited to solution concentrations less than ~0.2-mole fraction because of the uncertainty in quantifying the weak ν_{OH} Raman scattering.

Figure 5. Raman spectra of the nitrile stretching region for 0.045 mole-fraction acetonitrile solutions. a) The bulk solution spectrum. b) Total scattering from a bare silica particle (black)

with solution phase (green) and silanol-associated (blue) component spectra. c) Total scattering from a C_{18}-silica particle (black), with the solution contribution (green), silica contribution (blue) and C_{18}-associated component of ν_{CN} (red). Data are plotted and difference spectra are determined as discrete points. Gaussian fits (solid lines) are used to determine amplitudes, peak widths, and center frequencies. Spectra are acquired with 3-cm^{-1} resolution.

Figure 6. Interfacial-excess acetonitrile in bare silica particles. Bulk solution-scattering of acetonitrile (▪) is compared with the scattering of acetonitrile from the silica surface (▲).

Figure 7. Interfacial-excess acetonitrile in C_{18}-silica particles. Bulk solution-scattering of acetonitrile (▪) is compared with the scattering of total excess acetonitrile from the C_{18} –silica interface (▪).

Figure 8. Distribution of interfacial acetonitrile between the C_{18}–chains (●) and surface silanols (▲).

Figure 9. The nitrile stretching frequency (ν_{CN}) of the acetonitrile from the bulk solution (▪), silanol associated acetonitrile (▲), and C_{18} associated acetonitrile (●) populations.

Figure 1

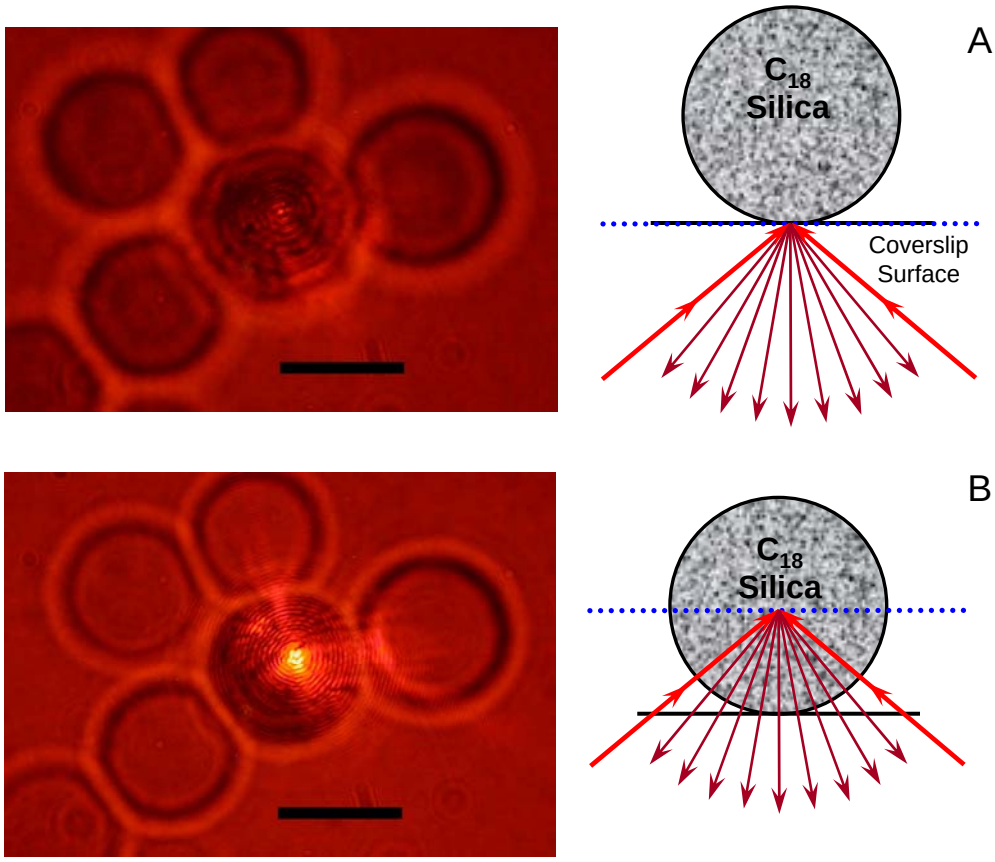

Figure 2

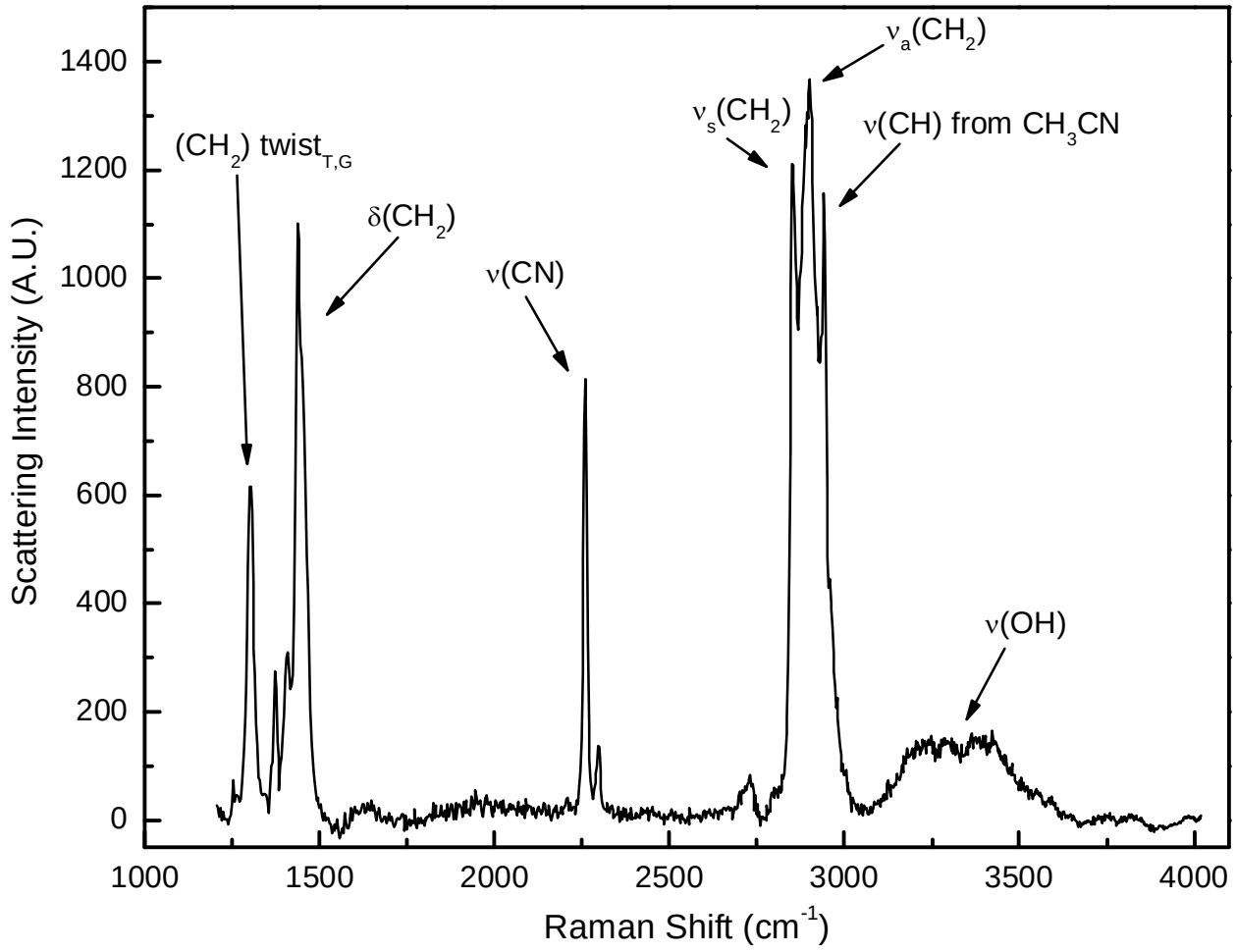
$\nu_a(CH_2)$
$\nu_s(CH_2)$
ν(CH) from CH_3CN
(CH_2) $twist_{T,G}$
$\delta(CH_2)$
ν(CN)
ν(OH)
Scattering Intensity (A.U.)
Raman Shift (cm^{-1})
0
200
400
600
800
1000
1200
1400
1000
1500
2000
2500
3000
3500
4000

Figure 3

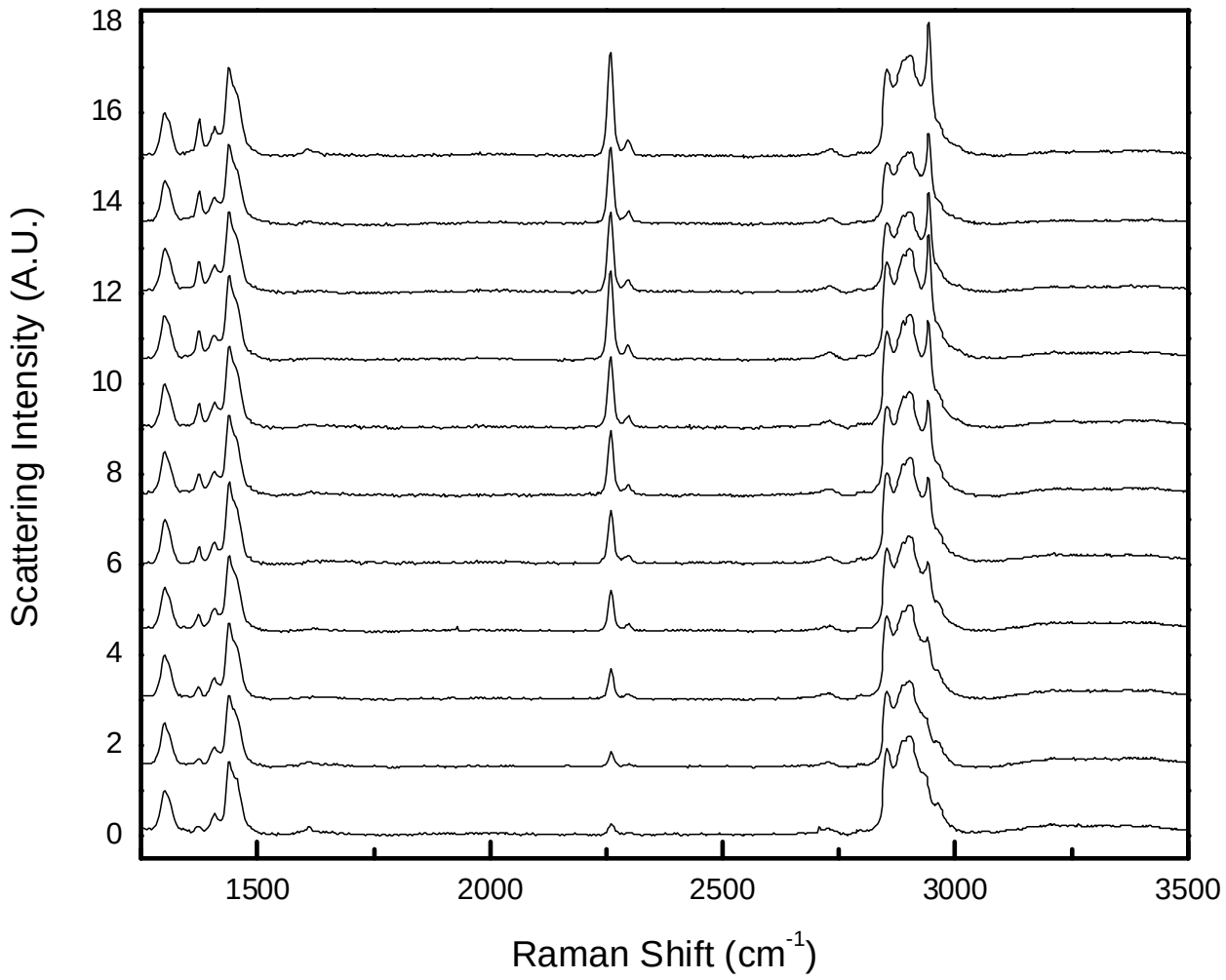
Scattering Intensity (A.U.)
0
2
4
6
8
10
12
14
16
18
1500
2000
2500
3000
3500
Raman Shift (cm-1)

Figure 4

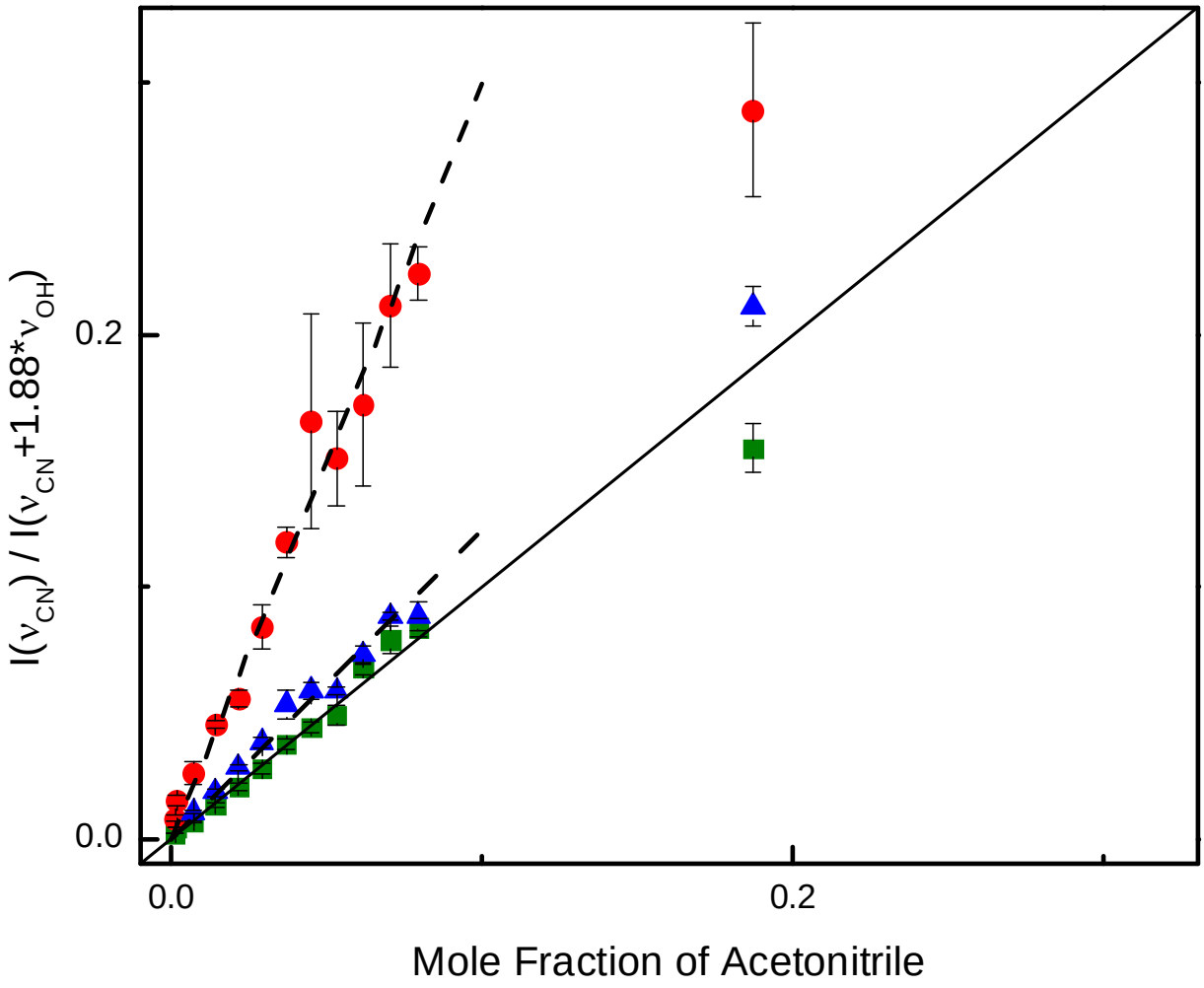

Figure 5

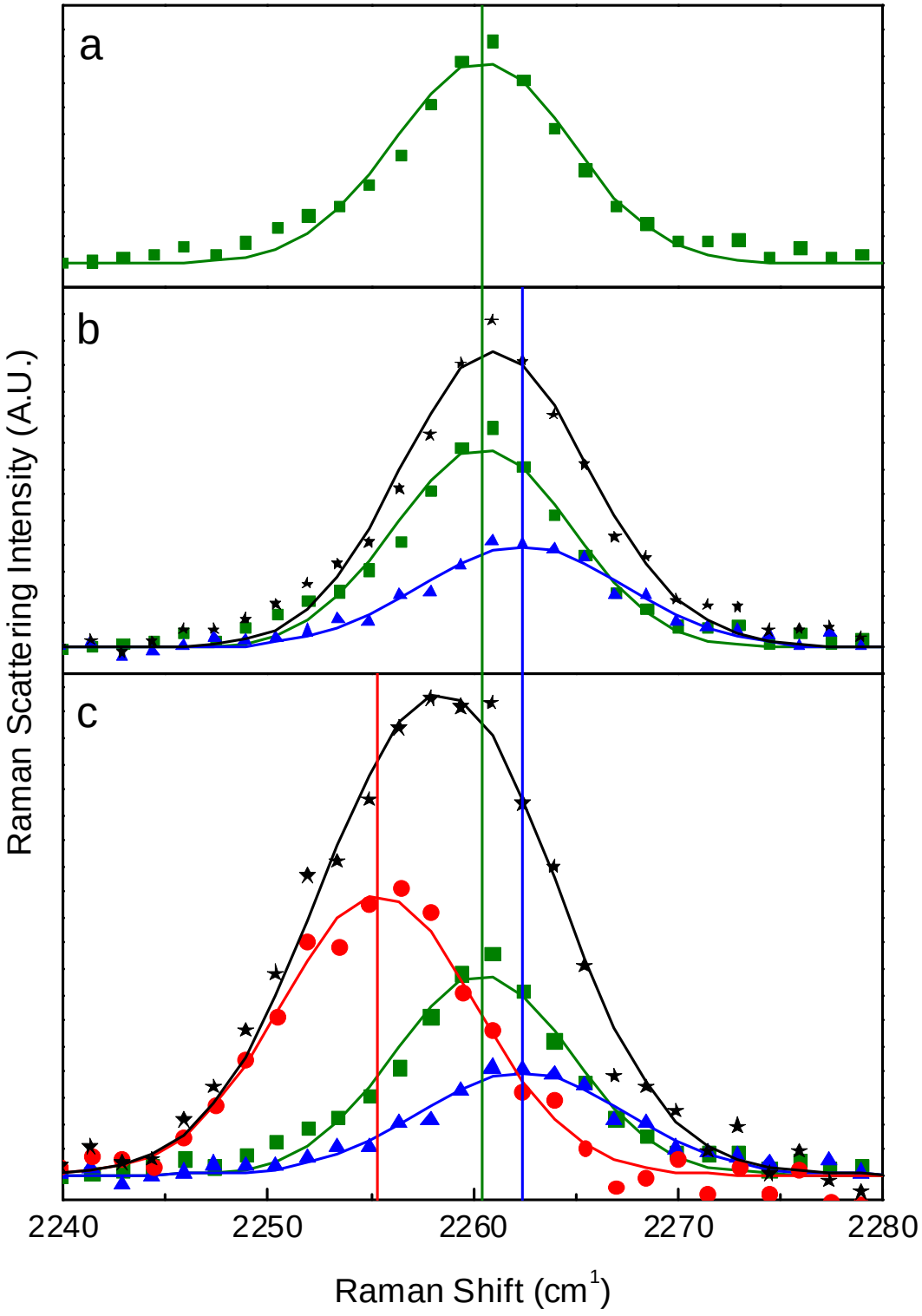
a
b
c
Raman Scattering Intensity (A.U.)
2240
2250
2260
2270
2280
Raman Shift (cm1)

Figure 6

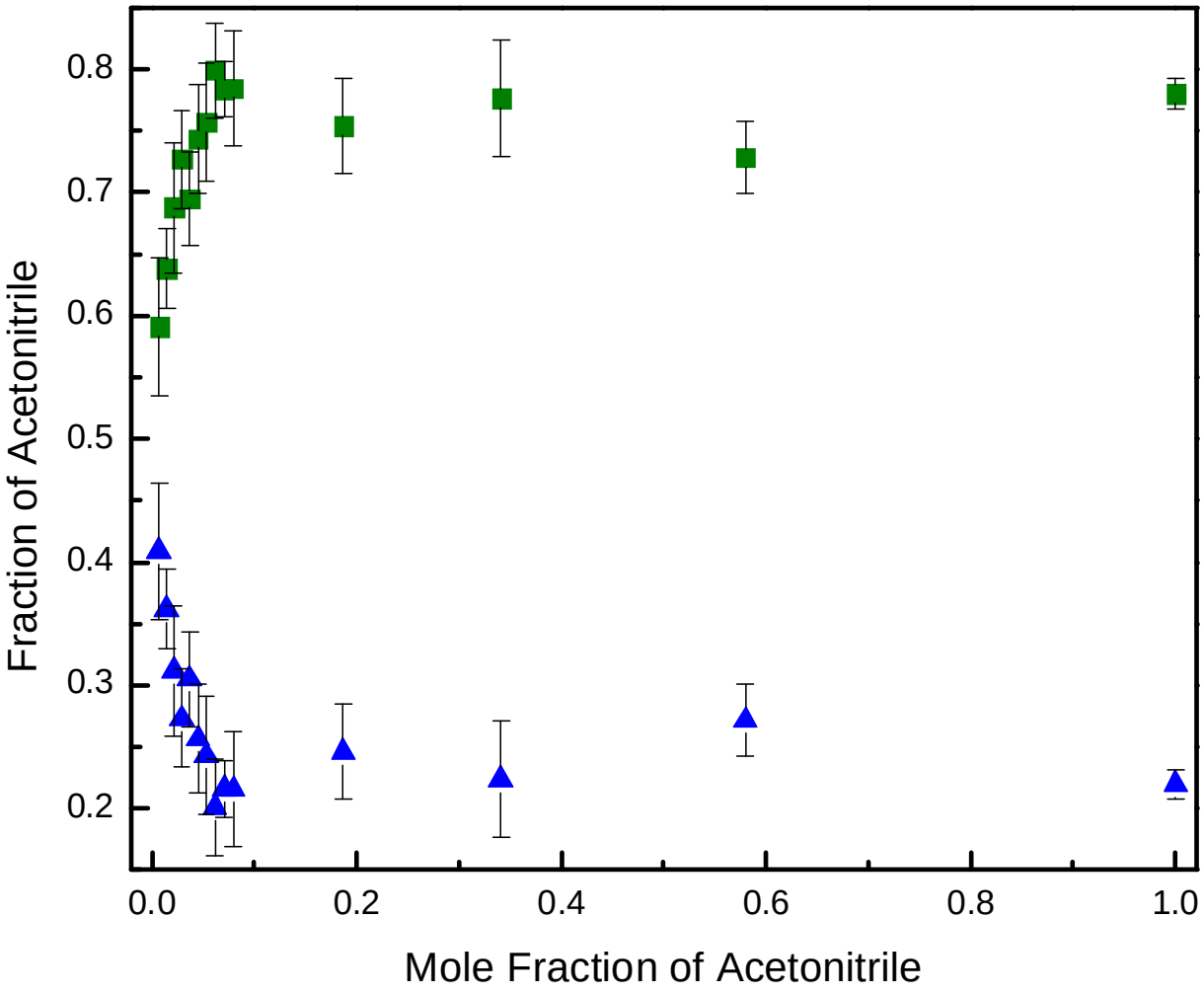
Fraction of Acetonitrile
0.2
0.3
0.4
0.5
0.6
0.7
0.8
0.0
0.2
0.4
0.6
0.8
1.0
Mole Fraction of Acetonitrile

Figure 7

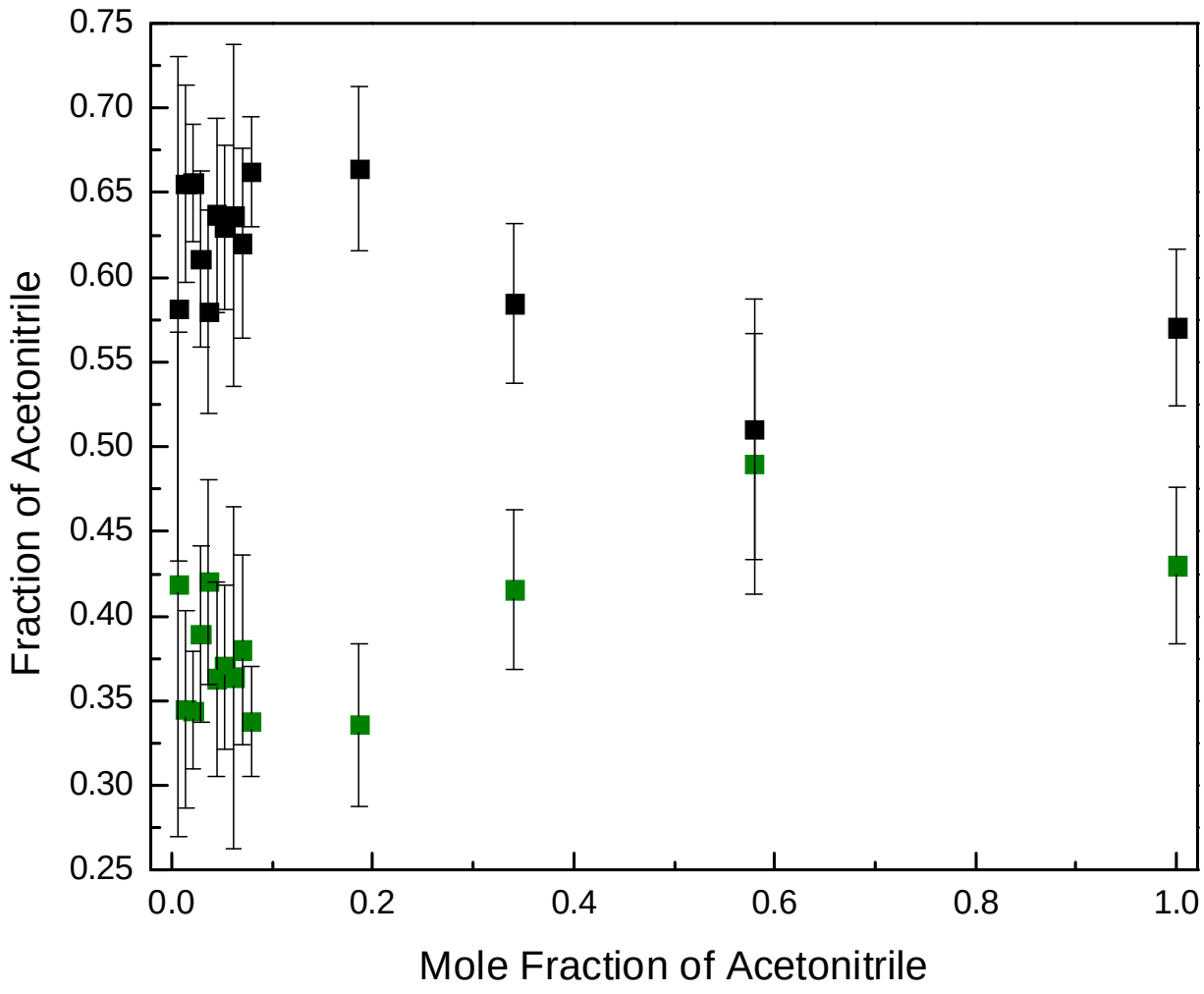
0.75
0.70
0.65
0.60
0.55
0.50
0.45
0.40
0.35
0.30
0.25
Fraction of Acetonitrile
0.0
0.2
0.4
0.6
0.8
1.0
Mole Fraction of Acetonitrile

Figure 8

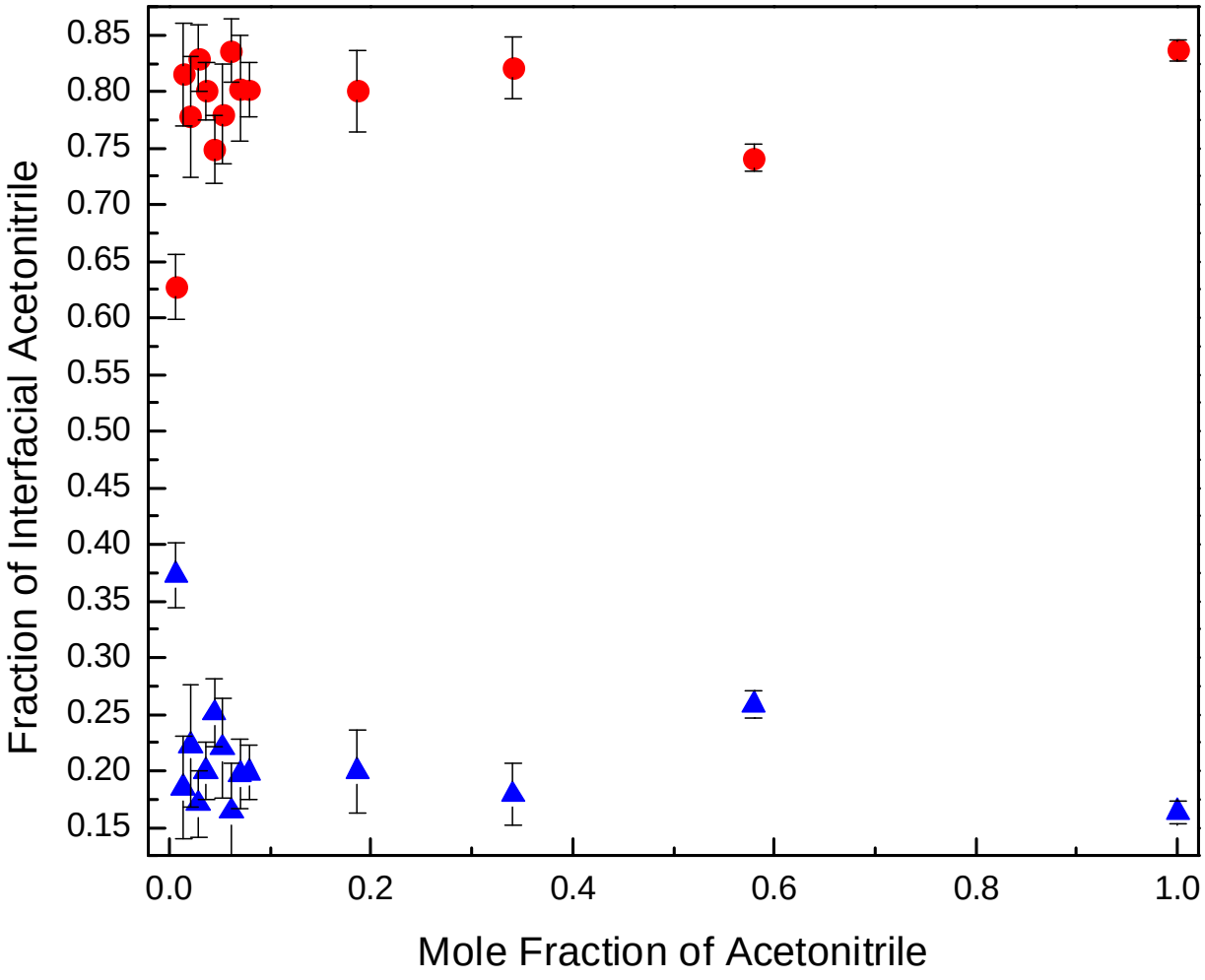
Fraction of Interfacial Acetonitrile
0.85
0.80
0.75
0.70
0.65
0.60
0.55
0.50
0.45
0.40
0.35
0.30
0.25
0.20
0.15
0.0
0.2
0.4
0.6
0.8
1.0
Mole Fraction of Acetonitrile

Figure 9

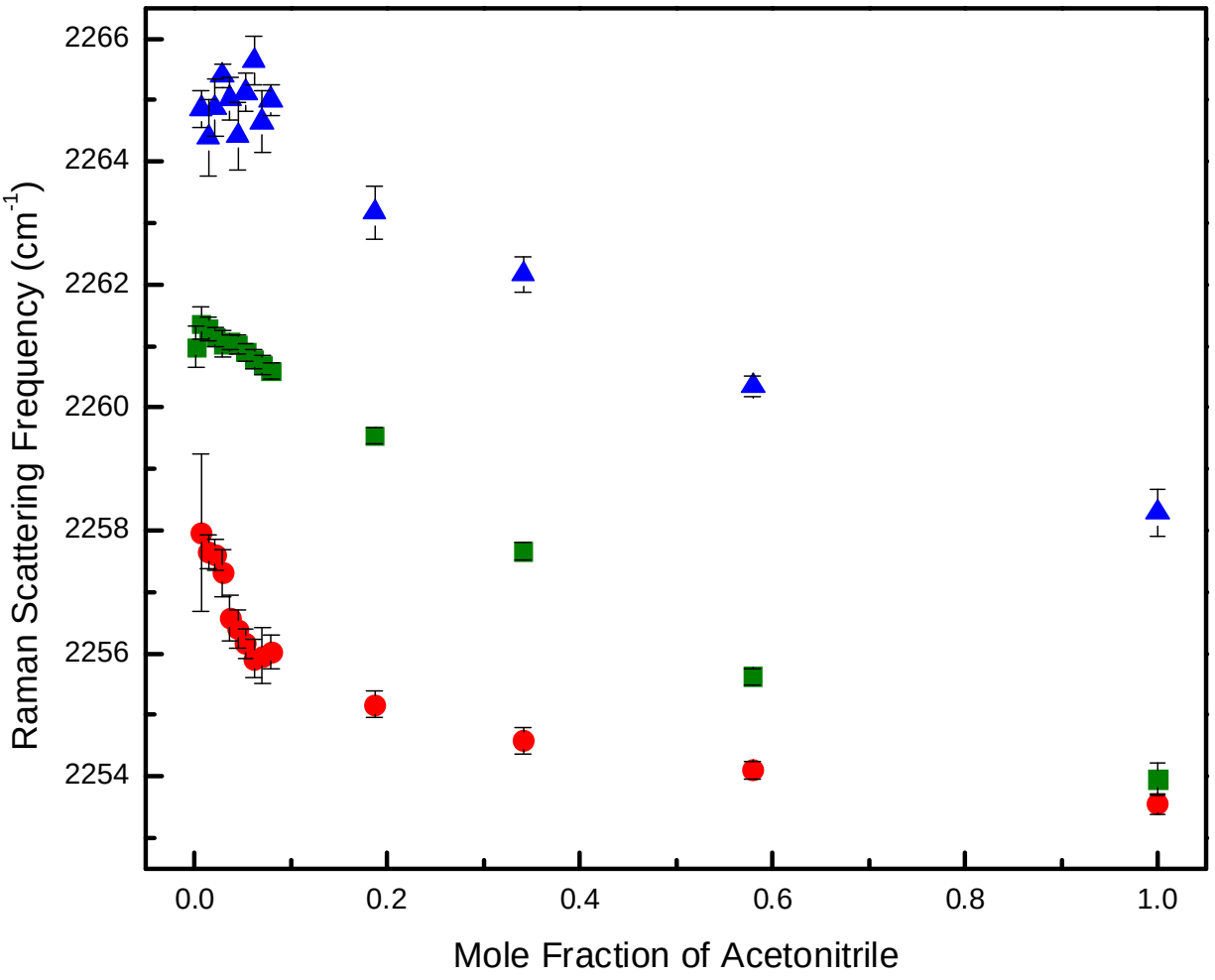
Raman Scattering Frequency (cm-1)
2266
2264
2262
2260
2258
2256
2254
0.0
0.2
0.4
0.6
0.8
1.0
Mole Fraction of Acetonitrile